Published in final edited form as:
Environ Pollut. 2018 September ; 240: 60–67. doi:10.1016/j.envpol.2018.04.085.

Light absorption of organic carbon emitted from burning wood, charcoal, and kerosene in household cookstoves

Mingjie Xie[1,2,3,4], **Guofeng Shen**[3,4], **Amara L. Holder**[4], **Michael D. Hays**[4], **James J. Jetter**[4]

[1]School of Environmental Science and Engineering, Nanjing University of Information Science & Technology, Nanjing 210044, China

[2]State Key Laboratory of Pollution Control and Resource Reuse, Nanjing University, Nanjing 210023, China

[3]Oak Ridge Institute for Science and Education (ORISE), Office of Research and Development, U.S. Environmental Protection Agency, 109 T.W. Alexander Drive, Research Triangle Park, NC 27711, USA

[4]National Risk Management Research Laboratory, Office of Research and Development, U.S. Environmental Protection Agency, 109 T.W. Alexander Drive, Research Triangle Park, NC 27711, USA

Abstract

Household cookstove emissions are an important source of carbonaceous aerosols globally. The light-absorbing organic carbon (OC), also termed brown carbon (BrC), from cookstove emissions can impact the Earth's radiative balance, but is rarely investigated. In this work, $PM_{2.5}$ filter samples were collected during combustion experiments with red oak wood, charcoal, and kerosene in a variety of cookstoves mainly at two water boiling test phases (cold start CS, hot start HS). Samples were extracted in methanol and extracts were examined using spectrophotometry. The mass absorption coefficients (MAC_{λ}, $m^2\ g^{-1}$) at five wavelengths (365, 400, 450, 500, and 550 nm) were mostly inter-correlated and were used as a measurement proxy for BrC. The MAC_{365} for red oak combustion during the CS phase correlated strongly to the elemental carbon (EC)/OC mass ratio, indicating a dependency of BrC absorption on burn conditions. The emissions from cookstoves burning red oak have an average MAC_{λ} 2–6 times greater than those burning charcoal and kerosene, and around 3–4 times greater than that from biomass burning measured in previous studies. These results suggest that residential cookstove emissions could contribute largely to

Correspondence to: Mingjie Xie (mingjie.xie@colorado.edu; 002902@nuist.edu.cn), Tel: +1-18851903788; Fax: +86-25-58731051; Mailing address: 219 Ningliu Road, Nanjing, Jiangsu, 210044, China.

Author contributions

M.X. and A.H. designed the research. M.X. performed the experiments. G.S. and J.J. managed sample collection. M.X. analyzed the data and wrote the paper with significant contributions from A.H., M.H., G.S. and J.J.

Competing financial interests

The authors declare no competing financial interests.

ambient BrC, and the simulation of BrC radiative forcing in climate models for biofuel combustion in cookstoves should be treated specifically and separated from open biomass burning.

Capsule

The radiative forcing of light-absorbing OC from cookstove emissions need to be considered in climate models, and should be treated separately from open biomass burning.

Keywords

Brown carbon; Cookstove combustion; Mass absorption coefficient; Burn condition

1 Introduction

Light-absorbing organic carbon (OC), also termed as “brown carbon” (BrC), directly affects the Earth’s radiative balance by absorbing incoming solar radiation (Ramanathan et al., 2001; Anderson et al., 2003; Bond and Begstrom, 2006). Unlike black carbon (BC) – the most efficient light absorbing agent, which absorbs across the spectral range with a weak dependence on wavelength (λ) (Bond, 2001; Bond et al., 2013; Lack and Langridge, 2013), BrC light absorption is mainly observed at near-UV and shorter visible wavelengths with a strong λ dependence (Kirchstetter et al., 2004; Laskin et al., 2015). Open biomass burning, including uncontrolled wildfire and prescribed agriculture or forest fires (Forrister et al., 2015; Washenfelder et al., 2015; Chakrabarty et al., 2016; Xie et al., 2017b), and biofuel use for household cooking and heating are significant primary sources of BrC (Zhang et al., 2016; Fleming et al., 2018). Additionally, a number of studies have investigated the formation of BrC through gas-phase photo-oxidation of volatile organic compounds (VOCs) from biogenic and anthropogenic sources (Iinuma et al., 2010; Nakayama et al., 2010; Updyke et al., 2012; Lambe et al., 2013; Lin et al., 2014; Liu et al., 2016; Xie et al., 2017a) and aqueous-phase photochemical processes (Powelson et al., 2014; Lin et al., 2015; De Haan et al., 2017), suggesting the existence of secondary BrC sources. Other potential BrC sources in urban areas, such as motor vehicle emissions, are rarely investigated (Xie et al., 2017b). Furthermore, the variability in the optical and chemical properties of BrC (e.g., spectral dependence and chromophore composition) from different sources is poorly characterized. Ambient and laboratory observations of BrC showed that compared with the water-soluble fraction of OC, the water-insoluble fraction contained more and stronger light-absorbing chromophores (Chen and Bond, 2010; Liu et al., 2013; Zhang et al., 2013; Cheng et al., 2016). The light absorption of biomass burning BrC is strongly dependent on burning conditions (e.g., temperature) (Chen and Bond, 2010; Saleh et al., 2014; Pokhrel et al., 2016; Xie et al., 2017b), and the majority of water extracts absorption was due to high molecular weight (> 500 Da) components (Di Lorenzo and Young, 2016; Di Lorenzo et al., 2017; Wong et al., 2017).

Residential solid fuels (e.g., wood, coal) were burned during cooking and heating activities in developing countries, of which the smoke emissions are a leading human health risk factor (Smith and Mehta, 2003; WHO, 2009, 2014). In Asia and Africa, approximately 60 – 80% of the BC emissions are from residential solid fuel (e.g., coal and biomass) combustion

(Cao et al., 2006; Bond et al., 2013); the emissions from residential solid fuels were estimated to contribute ~20% to the global OC budget (Bond et al., 2004). Solid fuel combustions in cookstoves can emit substantial particulate and gaseous pollutants, including $PM_{2.5}$, BC, OC, CO, NO_X, and SO_2 (Zhang et al., 2000). The emission factors (EFs) of these pollutants from household cookstoves have been intensively examined (Jetter et al., 2012; Shen et al., 2012, 2017, 2018; Qi et al., 2017; Wathore et al., 2017), aiming to reduce pollutant emissions by using improved cookstoves or clean fuels or a combination of them. However, the contribution of cookstove emissions to residential emissions is poorly constrained, and the BrC absorption from cookstove emissions is rarely studied. Sun et al. (2017) studied the light-absorbing properties of BrC from residential coal combustion, and found that the light absorption of BrC (350 – 850 nm) accounts for 26.5% of the total absorption (BrC + BC), suggesting the importance of accounting for BrC emissions from household cookstove in climate models.

This study aims to measure the light absorption of BrC from a variety of fuel-cookstove combinations. Specifically, the mass absorption coefficients (MAC, $m^2\ g^{-1}$) of methanol-extracted OC in $PM_{2.5}$ samples from cookstove emissions were compared across three types of fuels: red oak, charcoal, and kerosene. No previous study has investigated the light absorption of OC from the combustion of charcoal and kerosene – two important fuels used for cooking and lighting in developing countries. The light absorption of gas-phase OC positive artifact (i.e., OC adsorbed on a backup quartz filter downstream of a polytetrafluoroethylene membrane filter for $PM_{2.5}$) is also presented, which might partly represent the light-absorbing properties of semivolatile gas-phase OC (Chen and Bond, 2010). This study will help increase the understanding of sources of light-absorbing OC emitted to the atmosphere. It also supports estimates of the direct radiative effect due to BrC from cookstove emissions.

2 Methods

2.1 Cookstove emissions test facility

The cookstove emission tests were conducted at the U.S. EPA cookstove test facility in Research Triangle Park, NC. Details of the facility design, test protocol, and pollutant measurement were provided elsewhere (Jetter and Kariher, 2009; Jetter et al., 2012). Briefly, cookstove emissions were routed into a stainless steel hood connected to a primary and secondary dilution tunnel. An induced-draft blower was used to provide filtered dilution air and hood air flows and maintain negative pressure through the entire system.

2.2 Fuels and cookstoves

As shown in Table S1, supplementary information, three fuels (red oak (*Quercus rubra*) wood, lump charcoal (not briquettes), and 1-K kerosene) were burned in cookstoves designed to burn each specific fuel. Wood and charcoal are typical solid fuels in developing countries (Bonjour et al., 2013); kerosene has been an important liquid household fuel since the mid-19^{th} century, and is widely used in developing countries for cooking and lighting (Lam et al., 2012). In this work, red oak is selected as representative biomass fuel ansed burned in five stoves. Both low (~10%) and high (~30%) moisture (on a wet weight basis)

oak fuels were burned in a Jiko Poa stove; only low moisture oak fuel was combusted in the four other wood stoves. The wood stoves tested in this work (Table S1) ranged from the traditional 3-stone fire to a forced-draft fan type cookstove (EcoChula XXL) (Jetter et al., 2012, Shen et al., 2017, 2018). Low moisture charcoal was combusted in five charcoal stoves, and Grade 1-K kerosene (ASTM, 2013) was burned in two cookstoves (Butterfly Model 2412 and 2668). Each fuel-cookstove combination was tested in triplicate.

2.3 Water boiling test (WBT) protocol

The WBT protocol (version 4) (Global Alliance for Clean Cookstoves, 2014) was applied to determine cookstove power, energy efficiency and fuel use. The WBT protocol includes three test phases: (1) cold-start (CS) high power phase begins with the cookstove, pot and water at ambient temperature; (2) hot-start (HS) high power phase immediately follows the CS phase with the cookstove hot but the pot and water at ambient temperature; and (3) low-power simmer phase (SIM) begins with the cookstove hot and the water temperature maintained 3 °C below the boiling point. A modified protocol was used for the charcoal stove, which was described in detail by Jetter et al. (2012). Continuous pollutant emission measurements and filter sampling were performed during each phase of the WBT protocol.

2.4 Emissions measurement and sampling

Gaseous pollutants, including CO, CO_2, CH_4, and total hydrocarbons (THC), were monitored continuously at the primary dilution tunnel using infrared and flame ionization detector (FID) analyzers (models 200, 300-HFID and 300MFID; California Analytical; Orange, CA). Background concentrations of gaseous pollutants were measured with real-time instruments at least 10 min before and after each test and were subtracted from test concentrations. Particulate matter with aerodynamic diameter ≤ 2.5 μm ($PM_{2.5}$) was sampled isokinetically on quartz-fiber filters (Qf) and polytetrafluoroethylene (PTFE) membrane filters positioned in parallel and downstream of $PM_{2.5}$ cyclones (URG; Chapel Hill, NC) at a flow rate of 16.7 L min^{-1}. The filter-based PM sampling was conducted in the primary dilution tunnel for low-emission fuel-cookstove combinations (e.g., forced-draft biomass stove), and in the secondary dilution tunnel for those with high emission (e.g., natural-draft biomass stove) to avoid overloading filters. In this study, $PM_{2.5}$ samples for red oak-EcoChula XXL and kerosene stoves were collected in the secondary dilution tunnel. A backup quartz-fiber filter (Qb) was installed downstream of the PTFE filter, to estimate the adsorption of gas-phase OC (a measure of "positive artifact") on the $PM_{2.5}$ sample. $PM_{2.5}$ mass (range 0.023 – 1.48 mg) was determined by measuring the PTFE filters gravimetrically with a microbalance (MC5, Sartorius, Germany) before and after sampling. OC and elemental carbon (EC) on Qf and Qb samples were measured using a thermal optical instrument (Sunset Laboratory, Portland, OR) and a revised NIOSH method 5040 (NIOSH, 1999), and no EC was observed on Qb samples. Cookstove test facility blank PTFE and quartz filters were also collected, and the associated $PM_{2.5}$ mass, OC and EC contamination were measured and subtracted from test samples. Filters were stored at ≤ −20 °C prior to solvent extraction and analysis.

2.5 Light absorption analysis

Details of the sample extraction, extraction efficiency calculation and light absorption analysis are provided in the supplementary information (Section 1). Briefly, an aliquot of each quartz filter sample was extracted with methanol and measured using a UV/Vis spectrometer after filtration. Field blanks were analyzed in a same manner for blank correction. In the current work, we focused on the light absorption of OC in $PM_{2.5}$ emitted at high power phases (CS and HS) with higher EFs of OC and EC than those at low power SIM phases. Details of the comparisons of EFs between high and low power WBT phases are provided in supplementary information (Section 2). The light-absorbing OC emitted at the SIM phase was only analyzed for the red oak-3 stone fire combination, as CS and HS phases are typically similar for the 3-stone fire. For ease of comparison, no SIM phase samples were analyzed for charcoal or kerosene combustion.

The amount of OC extracted from Qf and Qb (or extraction efficiency) are calculated basing on the difference between OC on the un-extracted sample and OC in the air-dried sample following extraction, which is required in subsequent data analysis for light absorption. In this work, the Qb samples contain relatively small amount of OC, ranging from 2.58 ± 1.57 μg cm^{-2} (mean ± standard deviation, charcoal combustion) to 5.12 ± 1.81 μg cm^{-2} (kerosene combustion). After extraction, the residual OC on Qb (not corrected with blanks, 0.53 ± 0.12 – 1.00 ± 0.64 μg cm^{-2}) is comparable to blank filters (0.67 ± 0.33 μg cm^{-2}) and no significant difference (Student's *t* test, $p > 0.05$) between them has been observed. As such, the variability in OC measurement of field blanks can impact the calculation of extraction efficiency of Qb substantially. Therefore, the extraction efficiency of Qb samples is assumed as 100% throughout this work.

2.6 Data analysis

The EC/OC (or BC-OC) ratio was a preferred indicator of fire conditions to modified combustion efficiency (MCE), defined as $CO_2/(CO_2 + CO)$ on a molar basis, in recent studies investigating BrC absorption (Saleh et al., 2014; Lu et al., 2015; Pokhrel et al., 2017; Xie et al., 2017b). Heat transfer efficiency (HTE) is the ratio of the heat used in cooking to heat released from combustion. The overall thermal efficiency (OTE) is the product of MCE and HTE and is an indication of stove energy efficiency. The EFs of OC and EC were calculated from the measured concentration, total volume of the exhaust, and burned fuel energy based on the total capture method (Shen et al., 2017). Details of the average MCE, OTE, and EFs (expressed per fuel energy, mg MJ^{-1}) of OC and EC for each fuel-stove combination are provided in Table S1 of the supplementary information. In this work, the measurement with value 0 among the triplicate tests was not used for average calculation, and the average value derived from less than three measurements was noted in each table.

To convert the light absorption of chromophores in solution to ambient aerosol chromophore concentrations, the light absorption (A_λ) of each sample extract measured by the UV/Vis spectrometer is converted to light absorption coefficient (Abs_λ, Mm^{-1}) by Eq.(1):

(Hecobian et al., 2010)

$$\mathrm{Abs}_{\lambda} = \left(A_{\lambda} - A_{700}\right) \times \frac{V_l}{V_a \times L} \ln(10) \quad (1)$$

where A_{700} (average ± standard deviation 0.0057 ± 0.013, range −0.0030 – 0.076) is subtracted from A_{λ} to account for systematic baseline drift (Zhang et al., 2013), V_l (m^3) is the volume of methanol (5 mL) used for extraction, V_a (m^3) is the volume of the sampled air represented by the extracted filter punch, and L (0.01 m) is the optical path length of the quartz cuvette in the UV/Vis spectrometer. The bulk mass absorption coefficient (MAC_{λ}, m^2 g^{-1}) was used to describe the absorption efficiency of extractable OC and calculated as (Eq. (2)):

(Zhang et al., 2013; Liu et al., 2016)

$$\mathrm{MAC}_{\lambda} = \frac{\mathrm{Abs}_{\lambda}}{C_{OC}} \quad (2)$$

where C_{OC} is the mass concentration of extracted OC for each filter sample (μg m^{-3}). In this work, MAC_{λ} at five representative wavelengths (λ = 365, 400, 450, 500, and 550 nm) were calculated. The solution absorption Ångström exponent ($Å_{abs}$), a measure of spectral dependence of light absorption, is determined from the slope of linear regression of $\log_{10}(\mathrm{Abs}_{\lambda})$ vs. $\log_{10}(\lambda)$ over the λ range of 300 and 550 nm. The average EC/OC ratio, extraction efficiency, MAC_{λ} and $Å_{abs}$ values of each fuel-cookstove combination for Qf samples are listed in Table S2; the ratio of OC on Qb sample (OC_{Qb}) and that on Qf sample (OC_{Qf}), MAC_{λ} and $Å_{abs}$ values of each fuel-cookstove combination for Qb samples are provided in Table S3.

As shown in Fig. S1, OC_{Qb} is positively related to OC_{Qf} and far from reaching maximum (saturation with gaseous organics) for most red oak and charcoal samples. The OC_{Qb} might also be partly composed of semi-volatile organics evaporated from the PTFE $PM_{2.5}$ filter ("negative artifact"). In this work, the Qb sample measurement was used as an upper limit of "positive artifact". The adjusted EC/OC ratio [$(EC/OC)_A$] was calculated as (Eq.(3)):

$$(\mathrm{EC/OC})_{\mathrm{A}} = \mathrm{EC}/\left(\mathrm{OC}_{\mathrm{Qf}} - \mathrm{OC}_{\mathrm{Qb}}\right) \quad (3)$$

The adjusted MAC_{λ} ($MAC_{\lambda,A}$, m^2 g^{-1}) is calculated by Eq.(4):

$$\mathrm{MAC}_{\lambda,\ A} = \frac{\mathrm{Abs}_{\lambda,Qf} - \mathrm{Abs}_{\lambda,Qb}}{\mathrm{C}_{\mathrm{OC,Qf}} - \mathrm{C}_{\mathrm{OC,Qb}}} \quad (4)$$

where $\mathrm{Abs}_{\lambda,Qf}$ and $\mathrm{Abs}_{\lambda,Qb}$ are light absorption coefficients of Qf and Qb extracts, $C_{\mathrm{OC,Qf}}$ and $C_{\mathrm{OC,Qb}}$ are extractable OC of Qf and Qb, here $C_{\mathrm{OC,Qb}}$ equals to $\mathrm{OC}_{\mathrm{Qb}}$ (assume 100%

extraction efficiency). The adjusted absorption Ångström exponent ($Å_{abs,A}$) was determined from the slope of linear regression of $\log_{10}(Abs_{\lambda,Qf} - Abs_{\lambda,Qb})$ vs. $\log_{10}(\lambda)$ over the λ range of 300 and 550 nm. The average $(EC/OC)_A$, MAC_λ and $Å_{abs,A}$ values for each fuel-cookstove combination are provided in Table S4.

3 Results and Discussion

3.1 Combustion Conditions and EFs across fuel-cookstove combinations.

3.1.1 Red oak—In Table S1, the MCE values for red oak burning in the five cookstoves are all higher than 90% at CS (range 95.6 ± 0.44 – 99.5 ± 1.64%) and HS/SIM (93.7 ± 0.5 – 99.5 ± 0.06%) phases, confirming that the combustion of red oak in different cookstoves is dominated by the flaming phase (Ferek et al., 1998). The Envirofit G3300 cookstove has the highest OTE and EFs of carbonaceous components (OC + EC) during both CS and HS phases. The combustion of high moisture red oak in the Jiko Poa has higher OC EFs ($p < 0.05$ for CS, $p > 0.05$ for HS), but lower EC EFs ($p < 0.05$) compared with combustion of low moisture red oak during both CS and HS phases.

3.1.2 Charcoal—Charcoal combustion in the five cookstoves is more flaming in CS phase (MCE 90.3 ± 0.5 – 97.3 ± 0.06%) than in HS phase (82.0 ± 2.14 – 95.2 ± 0.78%, Table S1). The OC EFs during the CS phase are less than 50% of those during the HS phase (except CH4400 cookstove). While the EC EFs decreased by more than 90% from the CS to HS phase. Except for the CH4400 cookstove, the variations of OC and EC EFs across different charcoal-cookstove combinations are smaller than the differences of EFs between CS and HS phases, suggesting that the initial temperature inside the cookstove plays an important role in determining the EC and OC emissions. The CS begins with all charcoal fuel at ambient temperature, while the HS begins with additional charcoal (at ambient temperature) added to hot charcoal remaining from the CS.

3.1.3 Kerosene—Kerosene combustion in the two cookstoves is flaming in the CS and HS phases (MCE > 90%, Table S1). The average OTE of the two kerosene-cookstove combinations (41.2 ± 0.96 – 49.5 ± 4.40%) are generally higher than red oak (22.9 ± 1.29 – 35.5 ± 0.86%) and charcoal (26.7 ± 1.87 – 46.0 ± 1.24%) cookstoves (Table S1). The OC and EC EFs for the Butterfly Model 2412 stove are more than 2–10 times higher than those for the Butterfly Model 2668 stove. Similar as red oak and charcoal combustions, the EFs of OC and EC are subject to large variability, which might be due to the small sample number for each fuel-cookstove combinations ($N = 3$) and the variability intrinsic to the combustion system.

3.2 Measurements of EC/OC ratio and light-absorbing properties

Due to the small sample population for each fuel-cookstove combination ($N = 3$), the measurements of EC/OC ratio and light absorption from cookstove OC emissions is grouped by fuel type and WBT phase. Typical MAC spectra of selected cookstove emissions samples for different WBT phases are shown in Fig. 1 and exhibit strong wavelength dependence ($Å_{abs} > 2$). Table S5 lists the average OCEC concentration, EC/OC ratio, OC extraction efficiency, MAC_λ, and $Å_{abs}$ values for Qf samples collected from burning red oak, charcoal,

and kerosene at CS and HS phases. The average OC concentration, OC_{Qb}/OC_{Qf} ratio, MAC_{λ}, and $Å_{abs}$ values of Qb are also provided.

3.2.1 Qf analysis—In Table S5, on average, higher EC/OC ratios are observed for the CS phase compared to the HS phase for the cookstoves burning charcoal (Student *t*-test, $p < 0.01$) and kerosene ($0.05 < p < 0.1$); red oak combustion has comparable EC/OC ratios between CS and HS phases, which was observed for most red oak-cookstove combinations in Table S2. This might be due to much lower EC EFs for HS phase for charcoal (0.24 ± 0.14 – 2.58 ± 0.31 mg MJ^{-1}) and kerosene (2.83 ± 0.51 – 6.03 ± 10.1 mg MJ^{-1}) combustion compared to those for CS phase (charcoal 60.8 ± 18.0 – 118 ± 62.4 mg MJ^{-1}, kerosene 3.80 ± 1.32 – 11.7 ± 6.26 mg MJ^{-1}; Table S1), while the OC EFs remain the same; the average OC and EC EFs are comparable between CS (OC 0.97 ± 0.21 – 68.3 ± 9.94 mg MJ^{-1}, EC 5.25 ± 1.16 – 114 ± 5.58 mg MJ^{-1}) and HS (OC 1.30 ± 0.58 – 135 ± 53.1 mg MJ^{-1}, EC 6.73 ± 0.40 – 166 ± 9.87 mg MJ^{-1}) phases for red oak combustion (Table S1). The average OC extraction efficiency from the cookstove samples is > 85% in this work, in agreement with the results of other studies on biomass burning emissions (Chen and Bond et al., 2010; Li et al., 2016; Xie et al., 2017b). The combustion of red oak generated the strongest light-absorbing OC among the three fuels during both CS (average $MAC_{365–550}$, 0.84 ± 0.98 – 5.09 ± 3.47 m^2 g^{-1}) and HS (0.58 ± 0.50 – 4.20 ± 2.18 m^2 g^{-1}) phases (Table S5). Except at λ = 365 nm, the MAC values at the other four wavelengths (400, 450, 500, 550 nm) are significantly higher ($p < 0.05$) for charcoal combustion during CS phase than HS phase. No significant MAC and $Å_{abs}$ difference ($p > 0.05$) is observed between CS and HS phases for red oak and kerosene combustion; although, the MAC values for red oak combustion are higher during the CS phase.

3.2.2 Qb analysis—Filters from kerosene combustion exhibit the largest relative adsorption artifact (OC_{Qb}/OC_{Qf}: CS 42.8 ± 15.2%, HS 69.3 ± 38.5%), followed by charcoal and red oak (Table S5). This is due to the fact that many of the Qb samples for kerosene combustion are nearly saturated with gaseous organics (Fig. S1), and the kerosene combustion has the highest OC concentrations for Qb samples (CS 150 ± 24.9 ug m^{-3}, HS 159 ± 79.9 ug m^{-3}, Table S5), but not for Qf samples (CS 430 ± 298 ug m^{-3}, HS 401 ± 431 ug m^{-3}). Red oak combustion also generated the strongest light-absorbing OC adsorbed on Qb during both CS (average $MAC_{365–550}$, 0.13 ± 0.08 – 1.96 ± 0.64 m^2 g^{-1}) and HS (0.20 ± 0.24 – 1.83 ± 1.79 m^2 g^{-1}) phases (Table S5), significantly higher ($p < 0.05$) than charcoal and kerosene combustion. Wood combustion likely generates relatively more aromatic compounds (e.g., phenols, PAHs) that absorb UV-visible radiation than charcoal combustion (Kim Oanh et al., 1999). The MAC_{λ} and $Å_{abs}$ values measured for Qb samples in Table S5 are comparable between CS and HS phases with no significant difference ($p > 0.05$) for all three fuel types. These results suggest that the light absorption of semi-volatile gas-phase OC from cookstove emissions is more sensitive to fuel type than the initial temperature inside the cookstove. Most of the average MAC_{λ} values for Qb samples are significantly lower ($p < 0.05$) than their corresponding Qf samples and exhibit stronger wavelength dependence (greater $Å_{abs}$ value, Table S5), indicating that the low-volatile organics on Qf are more light-absorbing than semi-volatile organics adsorbed on Qb, in accordance with the observations in Chen and Bond (2010).

3.2.3 Qf analysis with Qb correction—With the assumption that the OC adsorbed on Qb only represents the "positive artifact", the corrected EC/OC ratio, MAC_{λ} and $Å_{abs}$ for Qf samples (denoted by the subscript A) are shown in Table S5. The average $(EC/OC)_A$ values for kerosene (CS 1.29 ± 0.80, HS 0.88 ± 0.32) combustion are nearly two times greater than their corresponding EC/OC ratios of Qf samples. This is due to the highest OC_{Qb}/OC_{Qf} ratios for kerosene combustion (Table S5). Each average $MAC_{\lambda,A}$ value is higher than the corresponding average MAC_{λ} values of Qf samples for the three fuels, supporting that lower volatility OC from cookstove emissions contain stronger light-absorbing chromophores than gas-phase OC. However, the difference between MAC_{λ} before Qb correction and $MAC_{\lambda,A}$ is not significant ($p > 0.05$) for the combustion of red oak and charcoal in cookstoves. The average $Å_{abs,A}$ values are comparable to their corresponding $Å_{abs}$ of Qf samples with no significant difference ($p > 0.05$) for the three fuel types, indicating that the wavelength dependence of BrC absorption is more likely determined by the low-volatile OC in cookstove emissions.

3.2.4 Comparison to other studies—In this work, the MAC_{λ} and $Å_{abs}$ values obtained for Qf samples were compared to other studies on primary BrC sources. Few studies consider the impact of positive artifact on BrC absorption measurements (Chen and Bond, 2010). Our study shows that after "positive artifact" correction, no substantial change is observed for the average MAC_{λ} and $Å_{abs}$ values of OC from red oak and charcoal combustion. Several previous studies measured the light-absorbing properties of BrC from biomass burning using a similar method (UV/Vis analysis of methanol extracts) as this work. For example, Chen and Bond (2010) and Li et al. (2016) investigated the BrC absorption from wood and corn stalk pyrolysis, respectively, at temperatures from 210 °C to 360 °C, and obtained comparable ranges of MAC_{400} (wood 0.50 – 1.66 $m^2\ g^{-1}$; corn stalk 0.66 – 1.06 $m^2\ g^{-1}$) and $Å_{abs}$ (wood 6.90 – 11.4; corn stalk 7.00 – 7.70). They found that the light absorption of OC from wood or corn pyrolysis increased with temperature. Xie et al. (2017b) collected open biomass burning samples from both field and laboratory experiments with five different fuels, and obtained average MAC_{365} and $Å_{abs}$ of 1.27 ± 0.34 $m^2\ g^{-1}$ (range 0.90 – 2.22 $m^2\ g^{-1}$) and 7.03 ± 0.93 (4.43 – 8.84), respectively. Moreover, the BrC absorption of ambient $PM_{2.5}$ particles with or without biomass burning impacts were intensively studied, and the corresponding MAC_{365} of water/methanol extracts are mostly in the range of 0.1 – 1.8 $m^2\ g^{-1}$ (Hecobian et al., 2010; Zhang et al., 2011, 2013; Liu et al., 2013; Du et al., 2014; Yan et al., 2015; Cheng et al., 2011, 2016). In this study, the average MAC for red oak combustion in cookstoves at 365 nm (CS 5.09 ± 3.47 $m^2\ g^{-1}$, HS 4.20 ± 2.18 $m^2\ g^{-1}$, Table S5) or 400 nm (CS 3.57 ± 2.97 $m^2\ g^{-1}$, HS 2.87 ± 1.80 $m^2\ g^{-1}$) are around 3–4 times greater than open biomass burning (Xie et al., 2017b) and biomass pyrolysis (Chen and Bond, 2010; Li et al., 2016). The MCE values are comparable between red oak-cookstove combustion in this study (CS 97.8 ± 1.40%, HS 97.2 ± 2.23%) and open biomass burning (mostly > 90%) in Holder et al. (2016) and Pokhrel et al. (2016). While the EC/OC ratios obtained for red oak-cookstove combustion (this study: CS 1.74 ± 1.42, HS 1.96 ± 1.74) are much higher than open biomass burning (generally << 0.5) in previous work (McMeeking et al., 2009; Akagi et al., 2011; Pokhrel et al., 2016; Xie et al., 2017b). As such, we suspect that the burning of red oak in cookstoves may occur at higher temperatures and produce more flaming.

In recent modeling studies exploiting the radiative forcing of BrC (Feng et al., 2013; Wang et al., 2014), the optical properties of biomass burning BrC are obtained from previous laboratory or ambient measurement (e.g., Chen and Bond, 2010; Zhang et al, 2013; Liu et al., 2013), of which the BrC absorption are much lower than cookstove emissions in this work. Therefore, the biofuel combustion in cookstoves should be treated as a distinct BrC source and separated from open biomass burning in climate models. Light absorption measurements of OC from charcoal and kerosene burning have not been investigated before, to our knowledge. The average MAC_{365} obtained for charcoal (CS 2.23 ± 1.17 $m^2\ g^{-1}$, HS 1.74 ± 0.34 $m^2\ g^{-1}$) and kerosene (CS 2.15 ± 0.93 $m^2\ g^{-1}$, HS 2.15 ± 1.44 $m^2\ g^{-1}$) combustion in this work are higher than those in previous biomass burning and ambient studies. As such, the combustion of solid or liquid fuels in cookstoves can generate strong light-absorbing OC, which needs to be considered in climate models due to the large contribution to global OC from residential emissions (Bond et al., 2004, 2013; Cao et al., 2006).

3.3 Light absorption versus burn condition

Several studies have demonstrated that the light absorption of OC from biomass burning depends largely on burn conditions (Saleh et al., 2014; Pokhrel et al. 2016; Xie et al., 2017b), and the parameterization of light absorbing properties (e.g., absorption Ångström exponent) using EC/OC ratio is quantitatively superior than that using MCE (Pokhrel et al., 2016). In this work, the MAC_{365} was selected to represent the light absorption of OC from cookstove emissions, because the MAC_{λ} values obtained at the five different wavelengths (365 – 550 nm) are mostly inter-correlated ($p < 0.05$) for each fuel combustion during CS or HS phase (Table S6), and MAC_{365} always has the highest value. The weak correlations between MAC_{550} and other MAC values at λ = 365, 400, 450, and 500 nm for kerosene combustion are due to the limited sample size and the weak absorption of sample extracts at 550 nm. The relationships of MAC_{365} vs. MCE, $Å_{abs}$ vs. MCE, MAC_{365} vs. EC/OC and $Å_{abs}$ vs. EC/OC with/without Qb correction (“positive artifact”) are presented for the three fuel combustions during CS and HS phases in Figs. 2, S2, and S3. In Fig. 2, panels (a) and (b), the general trend of increasing MAC_{365} with increasing MCE suggests that the light absorption of OC from the combustion of red oak in cookstoves is dependent on burn conditions. However, the variability of MAC_{365} in the region with MCE value lower or higher than 99% is not dependent on MCE, although the linear correlation of MAC_{365} vs. MCE is significant ($p < 0.01$) for combustion during the CS phase. This might suggest that the MCE is not an appropriate parameter in predicting wood combustion in cookstoves. Unlike MAC_{365}, $Å_{abs}$ exhibited negative dependency on MCE, and the correlation is significant ($p < 0.01$), except for $Å_{abs}$ collected for HS phase with Qb correction.

In Fig. 2 panels (c) and (d), the EC/OC ratio varies by a factor of up to 30, while the corresponding MCE values have a variability of less than 10% (Fig. 2a,b), which might partly explain why the MAC_{365} can hardly be predicted by MCE. MAC_{365} is strongly correlated ($p < 0.01$) with EC/OC ratio during both CS and HS phases. However, the correlation of MAC_{365} vs. EC/OC for the HS phase is dominated by two samples collected for the red oak-EcoChula XXL combination (Fig. 2d). Most of the other data points in Fig. 2 panel (d) are clustered at the left bottom side, exhibiting no correlation between MAC_{365}

and EC/OC ratio ($r = 0.06$, $p > 0.05$). Red oak burned in the EcoChula XXL stove has the lowest average OC and EC EFs, but the highest average EC/OC ratio and MAC_{365} for all cookstoves with this fuel (Tables S1 and S2). Without considering the samples collected from the EcoChula XXL stove, the correlation of MAC_{365} vs. EC/OC for the CS phase combustion is still significant ($r = 0.73$, $p < 0.01$); the $Å_{abs}$ is inversely related to EC/OC ratio for both CS and HS phases. These results suggested that the EC/OC ratio is superior to MCE in predicting MAC_{λ} for burning of red oak during the CS phase. However, for burning of red oak during the HS phase, MAC_{λ} is more likely dependent on cookstove type, rather than the burn condition. In Fig. S2, the MAC_{365} and $Å_{abs}$ are weakly or not dependent on MCE or EC/OC ratio for charcoal combustion, and their variability is much lower than that of the EC/OC ratio. The emissions measurements presented may provide reasonable ranges of MAC_{λ} and $Å_{abs}$ for charcoal combustion in cookstoves. Due to the limited sample size, no conclusion can be drawn on the relationship between light-absorbing properties of OC and burn conditions for kerosene combustion emissions (Fig. S3).

4 Conclusions

This study measured the light absorption of methanol-extractable OC emitted from red oak, charcoal, and kerosene burning in a variety of cookstoves mainly at two WBT phases. Moreover, the light absorption of OC due to “positive artifact” is also examined as a proxy for semi-volatile, gas-phase OC. Consistent with previous studies, a negative dependency of $Å_{abs}$ has been observed with red oak burning conditions, as depicted by the relationship of $Å_{abs}$ vs. MCE and $Å_{abs}$ vs. EC/OC. We observe that the EC/OC ratio is more sensitive than MCE for predicting MAC_{365}. The MAC_{365} and $Å_{abs}$ may depend less on MCE or EC/OC ratio for charcoal and kerosene combustions. The light absorption of OC from cookstove emissions, as represented by MAC_{λ} values, are generally stronger than that from biomass burning in previous studies, and the correction of “positive artifact” does not change the light-absorbing characteristics substantially. Therefore, the radiative forcing of BrC from cookstove emissions might need to be considered in climate models, and the burning of biofuels in cookstoves should be treated separately from open biomass burning. Emissions characterized under various actual operating conditions in the field may be different than the emissions evaluated under the controlled laboratory conditions in this study.

Supplementary Material

Refer to Web version on PubMed Central for supplementary material.

Acknowledgments

This research was supported by the National Natural Science Foundation of China (NSFC, 41701551), the State Key Laboratory of Pollution Control and Resource Reuse Foundation (No. PCRRF17040), the Startup Foundation for Introducing Talent of NUIST, in part by an appointment to the Postdoctoral Research Program at the National Risk Management Research Laboratory administered by the Oak Ridge institute for Science and Education through Interagency Agreement No. 92433001 between the U.S. Department of Energy and the U.S. Environmental Protection Agency. We thank B. Patel for assistance on ECOC analysis of $PM_{2.5}$ filters. Data used in the writing of this manuscript can be obtained upon request to Mingjie Xie (mingjie.xie@colorado.edu; 002902@nuist.edu.cn).

References

Akagi SK, Yokelson RJ, Wiedinmyer C, Alvarado MJ, Reid JS, Karl T, Crounse JD, and Wennberg PO: Emission factors for open and domestic biomass burning for use in atmospheric models, Atmos. Chem. Phys, 11, 4039–4072, doi:10.5194/acp-11-4039-2011, 2011.

Anderson TL, Charlson RJ, Schwartz SE, Knutti R, Boucher O, Rodhe H, and Heintzenberg J: Climate forcing by aerosols--a hazy picture, Science, 300, 1103–1104, doi:10.1126/science.1084777, 2003. [PubMed: 12750507]

ASTM D3699–13be1, Standard Specification for Kerosene, ASTM International, West Conshohocken, PA, doi: 10.1520/D3699-13BE01, 2013.

Bond TC: Spectral dependence of visible light absorption by carbonaceous particles emitted from coal combustion, Geophys. Res. Lett, 28, 4075–4078, doi:10.1029/2001gl013652, 2001.

Bond TC, Streets DG, Yarber KF, Nelson SM, Woo J-H, and Klimont Z: A technology-based global inventory of black and organic carbon emissions from combustion, J. Geophys. Res. Atmos, 109, doi:10.1029/2003jd003697, 2004.

Bond TC, and Bergstrom RW: Light absorption by carbonaceous particles: An investigative review, Aerosol Sci. Technol, 40, 27–67, doi:10.1080/02786820500421521, 2006.

Bond TC, Doherty SJ, Fahey DW, Forster PM, Berntsen T, DeAngelo BJ, Flanner MG, Ghan S, Kärcher B, Koch D, Kinne S, Kondo Y, Quinn PK, Sarofim MC, Schultz MG, Schulz M, Venkataraman C, Zhang H, Zhang S, Bellouin N, Guttikunda SK, Hopke PK, Jacobson MZ, Kaiser JW, Klimont Z, Lohmann U, Schwarz JP, Shindell D, Storelvmo T, Warren SG, and Zender CS: Bounding the role of black carbon in the climate system: A scientific assessment, J. Geophys. Res. Atmos, 118, 5380–5552, doi:10.1002/jgrd.50171, 2013.

Bonjour S, Adair-Rohani H, Wolf J, Bruce NG, Mehta S, Prüss-Ustün A, Lahiff M, Rehfuess EA, Mishra V, and Smith KR: Solid fuel use for household cooking: Country and regional estimates for 1980–2010, Environ. Health Perspect, 121, 784–790, doi:10.1289/ehp.1205987, 2013. [PubMed: 23674502]

Cao G, Zhang X, and Zheng F: Inventory of black carbon and organic carbon emissions from China, Atmos. Environ, 40, 6516–6527, 10.1016/j.atmosenv.2006.05.070, 2006.

Chakrabarty RK, Gyawali M, Yatavelli RLN, Pandey A, Watts AC, Knue J, Chen LWA, Pattison RR, Tsibart A, Samburova V, and Moosmüller H: Brown carbon aerosols from burning of boreal peatlands: microphysical properties, emission factors, and implications for direct radiative forcing, Atmos. Chem. Phys, 16, 3033–3040, doi:10.5194/acp-16-3033-2016, 2016.

Chen Y, and Bond TC: Light absorption by organic carbon from wood combustion, Atmos. Chem. Phys, doi:10, 1773–1787, 10.5194/acp-10-1773-2010, 2010.

Cheng Y, He KB, Zheng M, Duan FK, Du ZY, Ma YL, Tan JH, Yang FM, Liu JM, Zhang XL, Weber RJ, Bergin MH, and Russell AG: Mass absorption efficiency of elemental carbon and water-soluble organic carbon in Beijing, China, Atmos. Chem. Phys, 11, doi:11497–11510, 10.5194/acp-11-11497-2011, 2011.

Cheng Y, He K. b., Du Z. y., Engling G, Liu J. m., Ma Y. l., Zheng M, and Weber RJ: The characteristics of brown carbon aerosol during winter in Beijing, Atmos. Environ, 127, 355–364, 10.1016/j.atmosenv.2015.12.035, 2016.

De Haan DO, Hawkins LN, Welsh HG, Pednekar R, Casar JR, Pennington EA, de Loera A, Jimenez NG, Symons MA, Zauscher M, Pajunoja A, Caponi L, Cazaunau M, Formenti P, Gratien A, Pangui E, and Doussin J-F: Brown carbon production in ammonium- or amine-containing aerosol particles by reactive uptake of methylglyoxal and photolytic cloud cycling, Environ. Sci. Technol, 51, 7458–7466, doi:10.1021/acs.est.7b00159, 2017. [PubMed: 28562016]

Di Lorenzo RA, and Young CJ: Size separation method for absorption characterization in brown carbon: Application to an aged biomass burning sample, Geophys. Res. Lett, 43, 458–465, doi: 10.1002/2015gl066954, 2016.

Di Lorenzo RA, Washenfelder RA, Attwood AR, Guo H, Xu L, Ng NL, Weber RJ, Baumann K, Edgerton E, and Young CJ: Molecular-size-separated brown carbon absorption for biomass-burning aerosol at multiple field sites, Environ. Sci. Technol, 51, 3128–3137, doi:10.1021/acs.est.6b06160, 2017. [PubMed: 28199090]

Du Z, He K, Cheng Y, Duan F, Ma Y, Liu J, Zhang X, Zheng M, and Weber R: A yearlong study of water-soluble organic carbon in Beijing II: Light absorption properties, Atmos. Environ, 89, 235–241, 10.1016/j.atmosenv.2014.02.022, 2014.

Feng Y, Ramanathan V, and Kotamarthi VR: Brown carbon: a significant atmospheric absorber of solar radiation?, Atmos. Chem. Phys, 13, 8607–8621, doi:10.5194/acp-13-8607-2013, 2013.

Ferek RJ, Reid JS, Hobbs PV, Blake DR, and Liousse C: Emission factors of hydrocarbons, halocarbons, trace gases and particles from biomass burning in Brazil, J. Geophys. Res. Atmos, 103, 32107–32118, 1998.

Fleming LT, Lin P, Laskin A, Laskin J, Weltman R, Edwards RD, Arora NK, Yadav A, Meinardi S, Blake DR, Pillarisetti A, Smith KR, and Nizkorodov SA: Molecular composition of particulate matter emissions from dung and brushwood burning household cookstoves in Haryana, India, Atmos. Chem. Phys, 18, 2461–2480, doi:10.5194/acp-18-2461-2018, 2018.

Forrister H, Liu J, Scheuer E, Dibb J, Ziemba L, Thornhill KL, Anderson B, Diskin G, Perring AE, Schwarz JP, Campuzano-Jost P, Day DA, Palm BB, Jimenez JL, Nenes A, and Weber RJ: Evolution of brown carbon in wildfire plumes, Geophys. Res. Lett, 42, 4623–4630, doi:10.1002/2015gl063897, 2015.

Global Alliance for Clean Cookstoves, 2014 Water Boiling Test (WBT) 4.2.3. Released 19 March 2014 http://cleancookstoves.org/technology-and-fuels/testing/protocols.html (accessed July 2017).

Hecobian A, Zhang X, Zheng M, Frank N, Edgerton ES, and Weber RJ: Water-Soluble Organic Aerosol material and the light-absorption characteristics of aqueous extracts measured over the Southeastern United States, Atmos. Chem. Phys, 10, 5965–5977, doi:10.5194/acp-10-5965-2010, 2010.

Holder AL, Hagler GSW, Aurell J, Hays MD, and Gullett BK: Particulate matter and black carbon optical properties and emission factors from prescribed fires in the southeastern United States, J. Geophys. Res. Atmos, 121, 3465–3483, doi:10.1002/2015jd024321, 2016.

Iinuma Y, Böge O, Gräfe R, and Herrmann H: Methyl-nitrocatechols: Atmospheric tracer compounds for biomass burning secondary organic aerosols, Environ. Sci. Technol, 44, 8453–8459, doi:10.1021/es102938a, 2010. [PubMed: 20964362]

Jetter J, Zhao Y, Smith KR, Khan B, Yelverton T, DeCarlo P, and Hays MD: Pollutant emissions and energy efficiency under controlled conditions for household biomass cookstoves and implications for metrics useful in setting international test standards, Environ. Sci. Technol, 46, 10827–10834, doi:10.1021/es301693f, 2012. [PubMed: 22924525]

Jetter JJ, and Kariher P: Solid-fuel household cook stoves: Characterization of performance and emissions, Biomass Bioenergy, 33, 294–305, 10.1016/j.biombioe.2008.05.014, 2009.

Kim Oanh NT, Bætz Reutergårdh L, and Dung NT: Emission of polycyclic aromatic hydrocarbons and particulate matter from domestic combustion of selected fuels, Environ. Sci. Technol, 33, 2703–2709, doi:10.1021/es980853f, 1999.

Kirchstetter TW, Novakov T, and Hobbs PV: Evidence that the spectral dependence of light absorption by aerosols is affected by organic carbon, J. Geophys. Res. Atmos, 109, D21208, doi:10.1029/2004jd004999, 2004.

Lack DA, and Langridge JM: On the attribution of black and brown carbon light absorption using the Ångström exponent, Atmos. Chem. Phys, 13, 10535–10543, doi:10.5194/acp-13-10535-2013, 2013.

Lam NL, Smith KR, Gauthier A, and Bates MN: Kerosene: A review of household uses and their hazards in low- and middle-income countries, J. Toxicol. Environ. Health, Part B, 15, 396–432, doi:10.1080/10937404.2012.710134, 2012.

Lambe AT, Cappa CD, Massoli P, Onasch TB, Forestieri SD, Martin AT, Cummings MJ, Croasdale DR, Brune WH, Worsnop DR, and Davidovits P: Relationship between oxidation level and optical properties of secondary organic aerosol, Environ. Sci. Technol, 47, 6349–6357, doi:10.1021/es401043j, 2013. [PubMed: 23701291]

Laskin A, Laskin J, and Nizkorodov SA: Chemistry of atmospheric brown carbon, Chem. Rev, 115, 4335–4382, doi:10.1021/cr5006167, 2015. [PubMed: 25716026]

Li X, Chen Y, and Bond TC: Light absorption of organic aerosol from pyrolysis of corn stalk, Atmos. Environ, 144, 249–256, 10.1016/j.atmosenv.2016.09.006, 2016.

Lin P, Laskin J, Nizkorodov SA, and Laskin A: Revealing brown carbon chromophores produced in reactions of methylglyoxal with ammonium sulfate, Environ. Sci. Technol, 49, 14257–14266, doi: 10.1021/acs.est.5b03608, 2015. [PubMed: 26505092]

Lin Y-H, Budisulistiorini SH, Chu K, Siejack RA, Zhang H, Riva M, Zhang Z, Gold A, Kautzman KE, and Surratt JD: Light-absorbing oligomer formation in secondary organic aerosol from reactive uptake of isoprene epoxydiols, Environ. Sci. Technol, 48, 12012–12021, doi:10.1021/es503142b, 2014. [PubMed: 25226366]

Liu J, Bergin M, Guo H, King L, Kotra N, Edgerton E, and Weber RJ: Size-resolved measurements of brown carbon in water and methanol extracts and estimates of their contribution to ambient fine-particle light absorption, Atmos. Chem. Phys, 13, 12389–12404, doi:10.5194/acp-13-12389-2013, 2013.

Liu J, Lin P, Laskin A, Laskin J, Kathmann SM, Wise M, Caylor R, Imholt F, Selimovic V, and Shilling JE: Optical properties and aging of light-absorbing secondary organic aerosol, Atmos. Chem. Phys, 16, 12815–12827, doi:10.5194/acp-16-12815-2016, 2016.

Lu Z, Streets DG, Winijkul E, Yan F, Chen Y, Bond TC, Feng Y, Dubey MK, Liu S, Pinto JP, and Carmichael GR: Light absorption properties and radiative effects of primary organic aerosol emissions, Environ. Sci. Technol, 49, 4868–4877, 10.1021/acs.est.5b00211, 2015. [PubMed: 25811601]

McMeeking GR, Kreidenweis SM, Baker S, Carrico CM, Chow JC, Collett JL, Hao WM, Holden AS, Kirchstetter TW, Malm WC, Moosmüller H, Sullivan AP, and Wold CE: Emissions of trace gases and aerosols during the open combustion of biomass in the laboratory, J. Geophys. Res. Atmos, 114, doi:10.1029/2009jd011836, 2009.

Nakayama T, Matsumi Y, Sato K, Imamura T, Yamazaki A, and Uchiyama A: Laboratory studies on optical properties of secondary organic aerosols generated during the photooxidation of toluene and the ozonolysis of α-pinene, J. Geophys. Res. Atmos, 115, doi:10.1029/2010jd014387, 2010.

NIOSH, 1999. National Institute of Occupational Safety and Health. Elemental carbon (diesel particulate): Method 5040, Rep. https://HYPERLINK "http://www.cdc.gov/niosh/docs/2003–154/pdfs/5040f3.pdf"www.cdc.gov/niosh/docs/2003-154/pdfs/5040f3.pdf (1999). Accessed July, 2017.

Pokhrel RP, Wagner NL, Langridge JM, Lack DA, Jayarathne T, Stone EA, Stockwell CE, Yokelson RJ, and Murphy SM: Parameterization of single-scattering albedo (SSA) and absorption Ångström exponent (AAE) with EC / OC for aerosol emissions from biomass burning, Atmos. Chem. Phys, 16, 9549–9561, doi:10.5194/acp-16-9549-2016, 2016.

Powelson MH, Espelien BM, Hawkins LN, Galloway MM, and De Haan DO: Brown carbon formation by aqueous-phase carbonyl compound reactions with amines and ammonium sulfate, Environ. Sci. Technol, 48, doi:985–993, 10.1021/es4038325, 2014. [PubMed: 24351110]

Qi J, Li Q, Wu J, Jiang J, Miao Z, and Li D: Biocoal briquettes combusted in a household cooking stove: Improved thermal efficiencies and reduced pollutant emissions, Environ. Sci. Technol, 51, 1886–1892, doi:10.1021/acs.est.6b03411, 2017. [PubMed: 28036164]

Ramanathan V, Crutzen PJ, Kiehl JT, and Rosenfeld D: Aerosols, climate, and the hydrological cycle, Science, 294, 2119–2124, doi:10.1126/science.1064034, 2001. [PubMed: 11739947]

Saleh R, Robinson ES, Tkacik DS, Ahern AT, Liu S, Aiken AC, Sullivan RC, Presto AA, Dubey MK, Yokelson RJ, Donahue NM, and Robinson AL: Brownness of organics in aerosols from biomass burning linked to their black carbon content, Nature Geosci, 7, 647–650, doi:10.1038/ngeo2220, 2014.

Shen G, Tao S, Wei S, Zhang Y, Wang R, Wang B, Li W, Shen H, Huang Y, Chen Y, Chen H, Yang Y, Wang W, Wei W, Wang X, Liu W, Wang X, and Simonich SLM: Reductions in emissions of carbonaceous particulate matter and polycyclic aromatic hydrocarbons from combustion of biomass pellets in comparison with raw fuel burning, Environ. Sci. Technol, 46, 6409–6416, doi: 10.1021/es300369d, 2012. [PubMed: 22568759]

Shen G, Preston W, Ebersviller SM, Williams C, Faircloth JW, Jetter JJ, and Hays MD: Polycyclic aromatic hydrocarbons in fine particulate matter emitted from burning kerosene, liquid petroleum gas, and wood fuels in household cookstoves, Energy Fuels, 31, 3081–3090, doi:10.1021/acs.energyfuels.6b02641, 2017. [PubMed: 30245546]

Shen G, Hays MD, Smith KR, Williams C, Faircloth JW, and Jetter JJ: Evaluating the performance of household liquefied petroleum gas cookstoves, Environ. Sci. Technol, 52, 904–915, 10.1021/acs.est.7b05155, 2018. [PubMed: 29244944]

Smith KR, and Mehta S: The burden of disease from indoor air pollution in developing countries: comparison of estimates, Int. J. Hyg. Environ. Health, 206, 279–289, 10.1078/1438-4639-00224, 2003. [PubMed: 12971683]

Sun J, Zhi G, Hitzenberger R, Chen Y, Tian C, Zhang Y, Feng Y, Cheng M, Cai J, Chen F, Qiu Y, Jiang Z, Li J, Zhang G, and Mo Y: Emission factors and light absorption properties of brown carbon from household coal combustion in China, Atmos. Chem. Phys, 17, 4769–4780, doi:10.5194/acp-17-4769-2017, 2017.

Updyke KM, Nguyen TB, and Nizkorodov SA: Formation of brown carbon via reactions of ammonia with secondary organic aerosols from biogenic and anthropogenic precursors, Atmos. Environ, 63, 22–31, 10.1016/j.atmosenv.2012.09.012, 2012.

Wang X, Heald CL, Ridley DA, Schwarz JP, Spackman JR, Perring AE, Coe H, Liu D, and Clarke AD: Exploiting simultaneous observational constraints on mass and absorption to estimate the global direct radiative forcing of black carbon and brown carbon, Atmos. Chem. Phys, 14, 10989–11010, doi:10.5194/acp-14-10989-2014, 2014.

Washenfelder RA, Attwood AR, Brock CA, Guo H, Xu L, Weber RJ, Ng NL, Allen HM, Ayres BR, Baumann K, Cohen RC, Draper DC, Duffey KC, Edgerton E, Fry JL, Hu WW, Jimenez JL, Palm BB, Romer P, Stone EA, Wooldridge PJ, and Brown SS: Biomass burning dominates brown carbon absorption in the rural southeastern United States, Geophys. Res. Lett, 42, 653–664, doi:10.1002/2014gl062444, 2015.

Wathore R, Mortimer K, and Grieshop AP: In-use emissions and estimated impacts of traditional, natural- and forced-draft cookstoves in rural Malawi, Environ. Sci. Technol, 51, 1929–1938, doi:10.1021/acs.est.6b05557, 2017. [PubMed: 28060518]

WHO: World Health Organization, Global Health Risks: Mortality and Burden of Disease Attributable to Selected Major Risks, World Health Organization: Geneva, Switzerland, 2009.

WHO: World Health Organization. Burden of disease from household air pollution for 2012, http://www.who.int/phe/health_topics/outdoorair/databases/en/ (accessed July 2017). 2014.

Wong JPS, Nenes A, and Weber RJ: Changes in light absorptivity of molecular weight separated brown carbon due to photolytic aging, Environ. Sci. Technol, 51, 8414–8421, 10.1021/acs.est.7b01739, 2017. [PubMed: 28640603]

Xie M, Chen X, Hays MD, Lewandowski M, Offenberg J, Kleindienst TE, and Holder AL: Light absorption of secondary organic aerosol: Composition and contribution of nitroaromatic compounds, Environ. Sci. Technol, 51, 11607–11616, doi:10.1021/acs.est.7b03263, 2017a. [PubMed: 28930472]

Xie M, Hays MD, and Holder AL: Light-absorbing organic carbon from prescribed and laboratory biomass burning and gasoline vehicle emissions, Sci. Rep, 7, 7318, doi:10.1038/s41598-017-06981-8, 2017b. [PubMed: 28779152]

Yan C, Zheng M, Sullivan AP, Bosch C, Desyaterik Y, Andersson A, Li X, Guo X, Zhou T, Gustafsson Ö, and Collett JL: Chemical characteristics and light-absorbing property of water-soluble organic carbon in Beijing: Biomass burning contributions, Atmos. Environ, 121, 4–12, 10.1016/j.atmosenv.2015.05.005, 2015.

Zhang J, Smith KR, Ma Y, Ye S, Jiang F, Qi W, Liu P, Khalil MAK, Rasmussen RA, and Thorneloe SA: Greenhouse gases and other airborne pollutants from household stoves in China: a database for emission factors, Atmos. Environ, 34, 4537–4549, 10.1016/S1352-2310(99)00450-1, 2000.

Zhang X, Lin Y-H, Surratt JD, and Weber RJ: Sources, composition and absorption Ångström exponent of light-absorbing organic components in aerosol extracts from the Los Angeles basin, Environ. Sci. Technol, 47, 3685–3693, doi:10.1021/es305047b, 2013. [PubMed: 23506531]

Zhang X, Lin Y-H, Surratt JD, Zotter P, Prévôt ASH, and Weber RJ: Light-absorbing soluble organic aerosol in Los Angeles and Atlanta: A contrast in secondary organic aerosol, Geophys. Res. Lett, 38, doi:10.1029/2011gl049385, 2011.

Zhang X, Kim H, Parworth CL, Young DE, Zhang Q, Metcalf AR, and Cappa CD: Optical properties of wintertime aerosols from residential wood burning in Fresno, CA: Results from DISCOVER-

AQ 2013, Environ. Sci. Technol, 50, 1681–1690, doi:10.1021/acs.est.5b04134, 2016. [PubMed: 26771892]

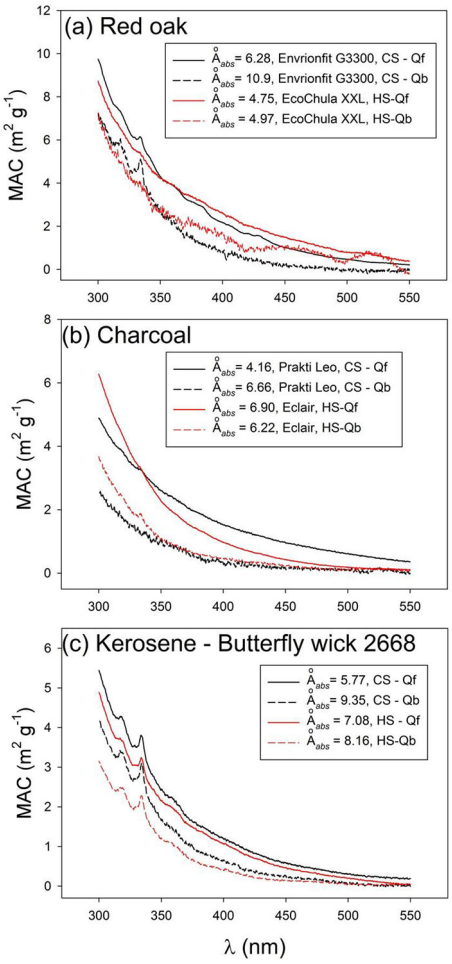

Fig. 1.

Typical MAC spectra of extracted OC from the combustion of (a) red oak, (b) charcoal and (c) kerosene in cookstoves during both CS and HS phases.

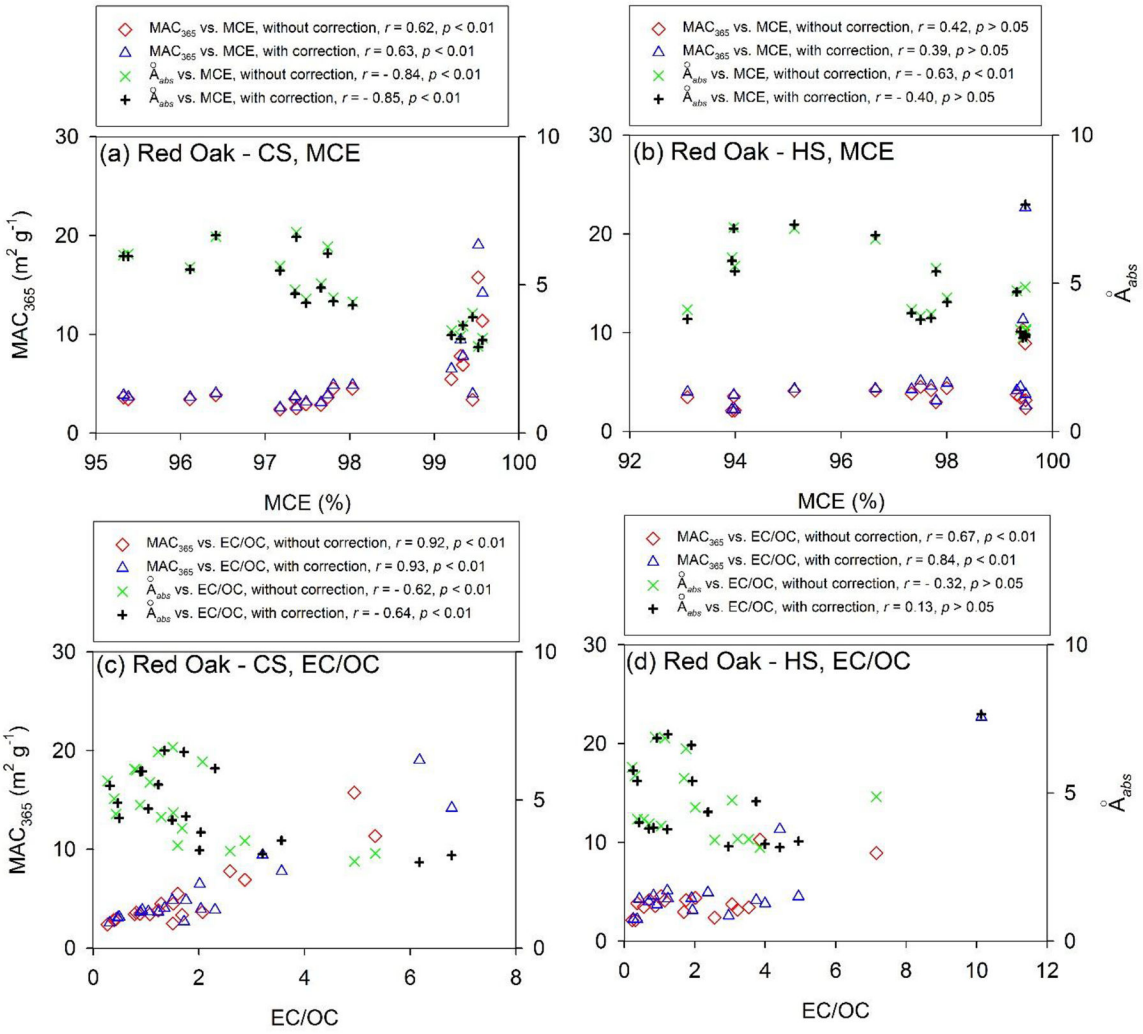

Fig. 2.

Relationships between MAC_{365} and (a) MCE during CS-phase, (b) MCE during HS-phase, (c) EC/OC ratio during CS-phase and (d) EC/OC ratio during HS-phase combustions of red oak in cookstoves with and without “positive artifact” corrections.